Protein Science (1994), *3*:2322-2339. Cambridge University Press. Printed in the USA.

The structures of RNase A complexed with 3′-CMP and d(CpA): Active site conformation and conserved water molecules

INGRID ZEGERS,[1] DOMINIQUE MAES,[1] MINH-HOA DAO-THI,[1]
FREDDY POORTMANS,[2] REX PALMER,[3] AND LODE WYNS[1]

[1] Institute of Molecular Biology, Vrije Universiteit Brussel, Paardenstraat 65, B-1640 St. Genesius Rode, Belgium
[2] VITO, Boeretang 200, B-2400 MOL, Belgium
[3] Birkbeck College, Malet Street, London WC1E 7HX, United Kingdom

(RECEIVED September 8, 1994; ACCEPTED October 25, 1994)

Abstract

The interactions of RNase A with cytidine 3′-monophosphate (3′-CMP) and deoxycytidyl-3′,5′-deoxyadenosine (d(CpA)) were analyzed by X-ray crystallography. The 3′-CMP complex and the native structure were determined from trigonal crystals, and the d(CpA) complex from monoclinic crystals. The differences between the overall structures are concentrated in loop regions and are relatively small. The protein–inhibitor contacts are interpreted in terms of the catalytic mechanism. The general base His 12 interacts with the 2′ oxygen, as does the electrostatic catalyst Lys 41. The general acid His 119 has 2 conformations (A and B) in the native structure and is found in, respectively, the A and the B conformation in the d(CpA) and the 3′-CMP complex. From the present structures and from a comparison with RNase T1, we propose that His 119 is active in the A conformation. The structure of the d(CpA) complex permits a detailed analysis of the downstream binding site, which includes His 119 and Asn 71. The comparison of the present RNase A structures with an inhibitor complex of RNase T1 shows that there are important similarities in the active sites of these 2 enzymes, despite the absence of any sequence homology. The water molecules were analyzed in order to identify conserved water sites. Seventeen water sites were found to be conserved in RNase A structures from 5 different space groups. It is proposed that 7 of those water molecules play a role in the binding of the N-terminal helix to the rest of the protein and in the stabilization of the active site.

Keywords: 3′-CMP complex; conserved solvent sites; d(CpA) complex; downstream binding; ribonuclease A mechanism; S-peptide

Bovine pancreatic ribonuclease (RNase A, EC 3.1.27.5) is a pyrimidine-specific ribonuclease, member of a large superfamily of homologous RNases (Beintema et al., 1988). The catalytic mechanism of RNase A has been studied in detail (Blackburn & Moore, 1982). Usher et al. (1972) have shown that the geometry of the transesterification step follows an in-line mechanism, requiring general base–general acid catalysis by 2 distinct groups located on either side of the phosphate. RNase A catalyzes the cleavage of RNA in 2 subsequent reactions. The first reaction is a transesterification, which results in the cleavage of the P-O5′ bond at the 3′ end of a pyrimidine, and the formation of a 2′,3′ cyclic nucleotide. This cyclic nucleotide can be hydrolyzed in a second reaction. Chemical modification studies (Crestfield et al., 1963; Hirs et al., 1965) and analysis of the pH dependence of the enzymatic activity (Findlay et al., 1962) have shown that 2 histidines and 1 lysine are essential for enzymatic activity. On the basis of NMR and crystallographic data, Roberts et al. (1969) proposed a model in which His 12 abstracts a proton from the 2′-oxygen that becomes a nucleophile and attacks the phosphorus, forming a penta-coordinated transition state. The 5′ leaving group is protonated by His 119, which acts as a general acid. It was postulated that Lys 41 forms a salt bridge with the negatively charged oxygens on the phosphorus and thereby sta-

Reprint requests to: Ingrid Zegers, Instituut Moleculaire Biologie, Dienst Ultrastructuur, Paardenstraat 65, B-1640 St. Genesius Rode, Belgium; e-mail: igzegers@vub.ac.be.

Abbreviations: 2′-CMP, cytidine 2′-monophosphate; 3′-CMP, cytidine 3′-monophosphate; 2′,5′-CpA, cytidyl-2′,5′-adenosine; 2′,5′-CpG, cytidyl-2′,5′-guanosine; d(CpG), deoxycytidyl-3′,5′-deoxyguanosine; d(CpA), deoxycytidyl-3′,5′-deoxyadenosine; 2′F-dUpA, 2′-deoxy, 2′-fluoro uridyl-3′,5′-adenosine; 3′-GMP, guanylyl 3′-monophosphate; Guo, guanosine; MPD, 2-methyl-2,4-pentanediol; O3-2′-CMP, 3-oxocytidine 2′-monophosphate; O8-2′-GMP, 8-oxo guanylyl 3′-monophosphate; UpcA, uridyl-3′,5′-(5′-deoxy, 5′-methylene)adenosine.

bilizes the transition state. The crystal structures of complexes of RNase A with the inhibitors 2′,5′-CpA (Wodak et al., 1977), 2′-CMP (Lisgarten et al., 1993), and with the transition-state analogue uridine vanadate (Wlodawer et al., 1983) confirm that His 12 and His 119 are located on either side of the phosphate site p1, and that the Lys 41 NZ group lies in the vicinity of the ribose-phosphate portion of the inhibitor.

There are still some difficulties, however, in the interpretation of the protein–inhibitor interactions in the crystal complexes of RNase A. First, in the complex with the transition-state analogue uridine vanadate, His 12 interacts with an equatorial oxygen and Lys 41 with the 2′-oxygen. This is the inverse from what would be expected if His 12 is the general base. A second problem is the conformation of the general acid His 119. In a phosphate complex of RNase A, Borkakoti et al. (1982) observed 2 distinct conformations (A and B) for His 119. Wlodawer et al. (1982, 1983) observed only conformation A, whereas in the semisynthetic RNase A described by Martin et al. (1987), His 119 mainly occupies position B. His 119 interacts with the phosphate in both conformations, and it is as yet not clear which conformation is catalytically active.

The nature of the downstream binding site of RNase A has recently been the subject of kinetic studies of mutants (Tarragona-Fiol et al., 1993). In order to compare the kinetic data with structural information, there is a need for high-resolution structures of dinucleotide complexes of RNase A. Previously published structures of dinucleotide complexes of RNase A (UpcA, Richards & Wyckoff, 1973; 2′,5′-CpA, Wodak et al., 1977; 2′F-dUpA, Pavlovsky et al., 1978) were not determined at high resolution nor extensively refined. The recently published, highly refined structures of the complexes of RNase A with 2′,5′-CpG and d(CpG) do not address this question because the inhibitors were found to be bound in a nonproductive way (Aguilar et al., 1991, 1992).

Thus, in order to clarify the protein–inhibitor interactions in RNase A, we determined the native structure and the 3′-CMP complex of RNase A from trigonal crystals and the complex of RNase A with d(CpA) from monoclinic crystals (Kinemage 1). The structures are interpreted in terms of the catalytic mechanism. Additionally, the solvent structure is compared to those of RNase A structures from all available space groups, and the role of conserved water sites is analyzed.

Results

Data collection and refinement

The trigonal crystals diffracted to a resolution of 2 Å, and data were collected to a resolution of 2.2 Å. The merging R for the native data set was low, indicating good quality data. The crystals that were soaked with 3′-CMP showed cracks, but diffracted well for 2–3 days. After a longer time, their quality diminished. The data of the 3′-CMP complex had a relatively high merging R (10.3%), but the data also had a high multiplicity and completeness, and the final data set yielded good electron density maps. The monoclinic crystals diffracted to very high resolution, and data were collected to 1.4 Å. Details about the refinement and the final structures are listed in Table 1.

The native trigonal structure of RNase A contained a tetrahedral anion in the active site, which was assumed to be a sulfate. The structure refined, without major structural adjustments, to an R-value of 15.8% for 1σ data. The final structure does not show any significant peaks in the $F_o - F_c$ difference density maps. The mean error of the coordinates as estimated by the method of Luzzati (1957) is 0.22 Å. The side chains of Lys 1, Lys 31, Arg 39, Gln 69, and His 119 had multiple conformations; the side chains of residues Ala 20–Asn 24, Gln 28, Lys 37, Lys 66, Ser 89, Lys 91, and Asn 94 had relatively weak electron densities; and there was no electron density for the side chain of Asn 34.

The electron density maps of the 3′-CMP complex of RNase A clearly showed the density corresponding to a 3′-CMP mol-

Table 1. *Details on data collection and refinement*

	Native (1RPH)	3′-CMP complex (1RPF)	d(CpA) complex (1RPG)
Space group	$P3_221$	$P3_221$	$P2_1$
Unit cell	$a = 64.75$ Å	$a = 65.25$ Å	$a = 30.00$
	$b = 64.75$ Å	$b = 65.25$ Å	$b = 38.27$
	$c = 65.21$ Å	$c = 65.52$ Å	$c = 53.17$
	$\alpha = \beta = 90°$, $\gamma = 120°$	$\alpha = \beta = 90°$, $\gamma = 120°$	$\alpha = \gamma = 90°$, $\beta = 106.0°$
Resolution range	10–2.2 Å	10–2.2 Å	10–1.4 Å
Completeness	93.3%	99.7%	91.0%
$R_{merge}(I)$	3.4%	10.3%	4.7%
No. measurements	16,249	43,289	92,138
No. unique reflections	7,698	8,395	20,881
Final R factor (1σ data)	15.8%	15.5%	17.2%
Mean error (Luzzati plot)	0.22 Å	0.22 Å	0.15 Å
Restraints information[a]			
Bond distance (Å)	0.016 (0.025)	0.018 (0.025)	0.017 (0.025)
Angle distance (Å)	0.027 (0.030)	0.033 (0.033)	0.032 (0.033)
Planar 1–4 distance (Å)	0.029 (0.025)	0.024 (0.025)	0.025 (0.025)
Planar RMS δ (Å)	0.013 (0.015)	0.016 (0.015)	0.012 (0.015)
Chiral center RMS δ (Å)	0.013 (0.018)	0.019 (0.018)	0.015 (0.018)

[a] Target restraints are given in parentheses.

ecule (Fig. 1). Some loop regions did not fit the electron density very well and had high temperature factors. These include backbone atoms of residues Ser 21 and Ser 89. Therefore, residues 18–23 and residues 88–91 were deleted from the model and rebuilt manually. After rebuilding, which entailed shifting the position of the atoms to up to an Å, both regions fitted the electron density better. Although residues Lys 1, Ser 21, Lys 66, Ser 89, Lys 91–Asn 94, Glu 111, and Asn 113 had weak electron density, no multiple conformations could be observed. Similar to the native structure, there was no density for the side chain of Asn 34. The 3′-CMP complex of RNase A refined to an *R*-value of 15.5, with a mean error of the coordinates of 0.22 Å as estimated by the method of Luzzati (1957).

The monoclinic d(CpA) complex refined without major structural adjustments to an *R*-value of 17.2%, with a mean error of the coordinates of 0.15 Å as determined by the method of Luzzati (1957). Two conformations were observed for the side chains of Ser 16, Ser 32, Leu 35, Lys 41, Asn 67, and Gln 69. The side chain of Asn 34, which is involved in packing contacts in this space group, is clearly visible in the electron density. The d(CpA) inhibitor was clearly defined (Fig. 1) and is bound with the phosphate moiety in the active site. The occupancies of the cytosine, phosphate moiety, and adenosine, when refined independently, were, respectively, 0.90, 0.91, and 0.91. A large electron density with an overall shape like an MPD molecule was filling a space between symmetry-related molecules. An MPD

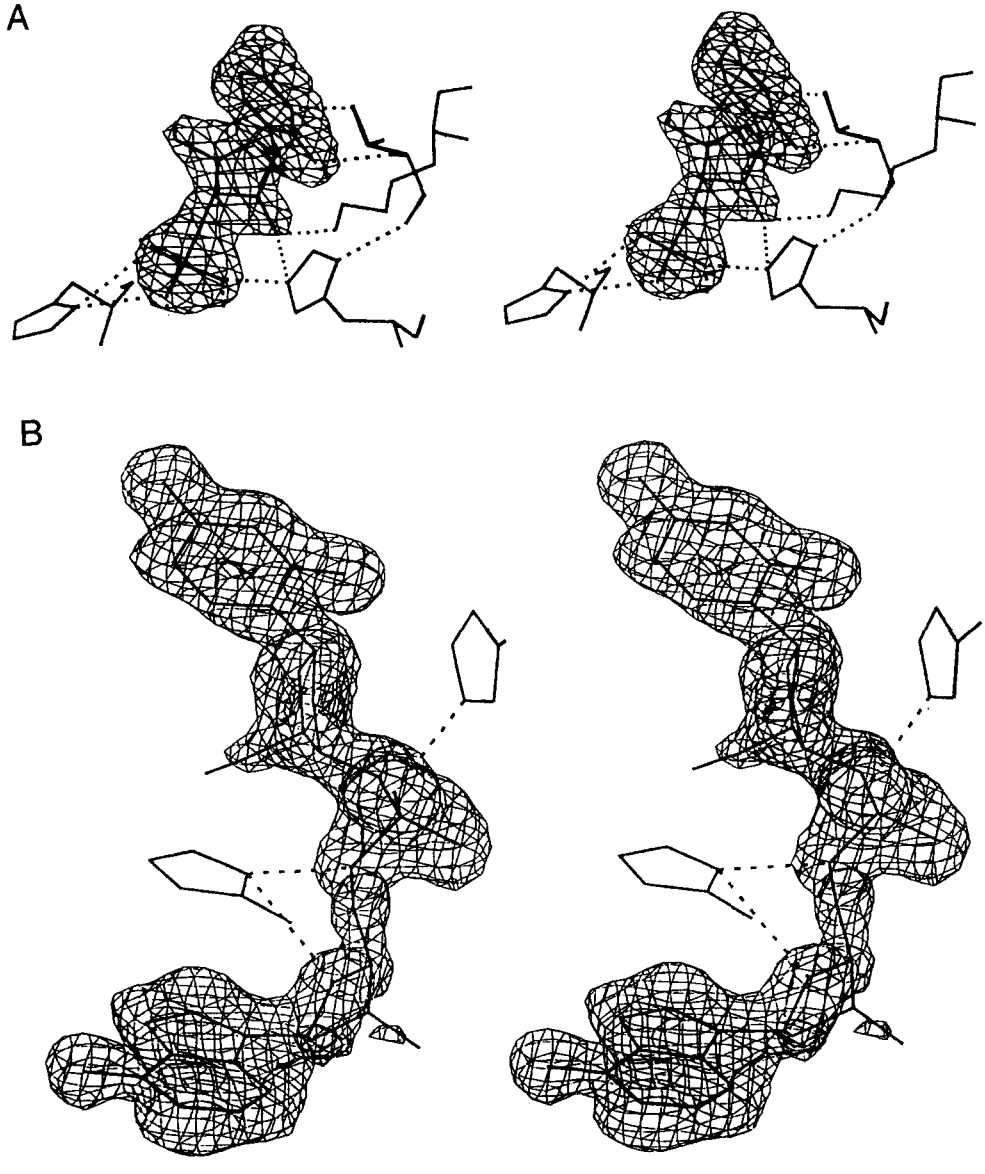

Fig. 1. Difference density of the inhibitors. $F_o - F_c$ difference density in the active site region of **(A)** RNase A * 3′-CMP and **(B)** RNase A * d(CpA). The structures were refined for 10 cycles after the inhibitors were removed from the coordinates. The refined inhibitors are shown, together with His 12, Lys 41, Thr 45, and His 119 (A) and His 12 and His 119 (B).

molecule in a single orientation was fitted into the electron density, but it is most probable that, in reality, the site is occupied by a mixture of stereoisomers in different orientations.

Overall structures

There are no major differences between the backbone atoms of the 3 structures presented here (Kinemage 1) and previously determined structures of RNase A (Table 2); the differences that are present are concentrated in loop regions, which are most variable in RNase A. The RMS difference between the 2 trigonal structures, the native RNase A and the 3′-CMP complex of RNase A, is 0.34 Å, which is slightly higher than the estimated error of the coordinates (0.22 Å). The differences between the 2 trigonal structures are concentrated in residues 19–23 and 87–91 (Fig. 2). These regions are also more variable in other RNase A structures, and the differences do not seem to be related to the presence or absence of an inhibitor. The packing of the trigonal and monoclinic structures are different. In the trigonal packing, RNase A forms a dimer, which is also found in all other high salt crystal forms of RNase A (Crosio et al., 1992). Because the RNase A used in the present work is unmodified, the present structures confirm that the dimerization is intrinsic to high salt conditions and not due to the covalent modifications present in all other high salt crystal structures. The largest differences between the trigonal structures on the one hand and the monoclinic d(CpA) complex on the other hand are found in the N-terminal region and the regions 35–42, 65–71, and 88–96. Regions 35–42 and 88–96 are loops that are situated in the same region of the protein, and have high temperature factors. These regions are also highly variable in other RNase A structures. The stretch comprising residues 65–71 is involved in the binding of the adenine in the monoclinic d(CpA) complex. In the monoclinic 2′-CMP complex of RNase A (Lisgarten et al., 1993), these residues are part of a hydrogen bonding network that stretches from the Gln 69 main-chain N over the side chains of Asn 67, Gln 69, and Asn 71 to the Cys 110 main-chain O. The atoms that participate in the network are well defined in the density and have low temperature factors. In the trigonal structures (native and 3′-CMP complex), this network has been disrupted despite the fact that residues 65–71 are not directly involved in inhibitor binding. In those 2 structures, 2 water molecules (Wat 192 and Wat 225) are in the center of a network linking Gln 69, Asn 71, and Glu 111. Gln 69 now has a relatively weak electron density and even 2 conformations in the native structure. Wat 225 is in contact with the active site residue His 119 in its B conformation. A similar arrangement, with a water in the same position as Wat 225 and His 119 in the B conformation, is also found in the orthorhombic structure of T-H12-RNase A (Nachman et al., 1990), in RNase S (Kim et al., 1992), and in the Asp 121 Asn mutant of RNase 1–118:111–124 (deMel et al., 1992). These structures have in common that they have been crystallized in high ionic strength conditions, but it is not clear how that could cause this specific arrangement.

Protein–inhibitor interactions

The active site of the native RNase A

In the structure of the native RNase A, a sulfate ion is bound in the active site (Fig. 4, Table 3), interacting with Gln 11, His 12, His 119, the backbone of Phe 120, and with 2 water molecules. Lys 41, identified as a catalytic residue by Findlay et al. (1962), does not interact with the sulfate and forms a hydrogen bond with Asn 44 instead. In general, the protein–sulfate interactions are similar to those found in the structure of Borkakoti et al. (1982) between the active site residues and a phosphate anion. The pyrimidine binding site B1 is occupied by the side chain of Lys 66 from a symmetry-related molecule and by 2 water molecules, one of which mimics the interaction of the cytidine N3 with Thr 45 OG1. During refinement of the structures presented here, special attention was paid to His 119, which has 2 conformations in the native structure (Kinemage 1). At the end of the refinement, the coordinates of the side-chain atoms of His 119 were deleted from the model and the structure refined for 9 cycles. The resulting difference map of the native RNase A (Fig. 3) still clearly shows 2 conformations for His 119. The 2 conformations correspond to the A and B conformations observed by

Table 2. *RNase A structures used for determining conserved water molecules*

Code[a]	Space group	Resolution (Å)	No. waters	*R*-value	Crystallization conditions	Remarks	Reference
1RPG	$P2_1$	1.4	164	17.2	pH 5.2, MPD	Cocrystallized with d(CpA)	Present work
7RSA	$P2_1$	1.26	188	15.0	pH 5.3, 2-methyl-2-propanol	Phosphate free	Wlodawer et al., 1988
1ROB	$P2_1$	1.6	101	17.0	pH 5.5, ethanol	Soaked with 2′-CMP	Lisgarten et al., 1993
1RPH	$P3_221$	2.2	99	15.8	pH 6, $(NH_4)_2SO_4$, NaCl	Sulfate in the active site	Present work
1RPF	$P3_221$	2.2	116	15.5	pH 6, $(NH_4)_2SO_4$, NaCl	Soaked with 3′-CMP	Present work
4SRN	$P3_221$	2.0	105	20.4	pH 5.2, $(NH_4)_2SO_4$, CsCl	Noncovalent complex of residues 1–118 and 111–124	Martin et al., 1987
1RSM	$P2_12_12_1$	2.0	75	18.0	pH 8.0, ethanol	Crosslinked Lys 7–Lys 41	Weber et al., 1985
2RNS	$P3_121$	1.6	88	17.6	pH 4.75, $(NH_4)_2SO_4$, CsCl	Cleavage between Ala 20 and Ser 21	Kim et al., 1992
8RSA	$P2_12_12_1$	1.77	246/2	16.2	pH 5.1, $(NH_4)_2SO_4$, CsCl	His 12 modified with deoxythymidine	Nachman et al., 1990

[a] The Protein Data Bank entry names are: PDBCode.ent.

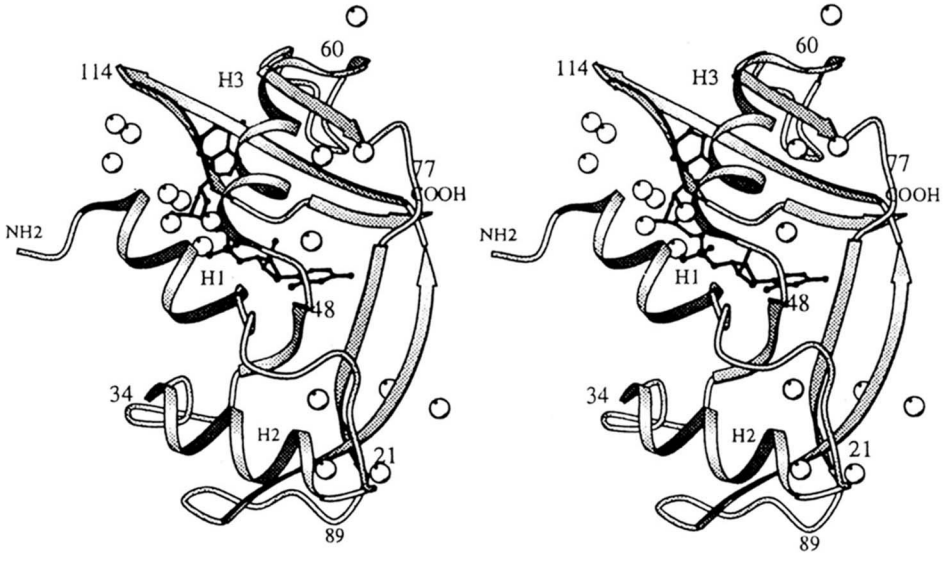

Fig. 2. Overall structure of RNase A. The overall structure of the d(CpA) complex of RNase A is shown as a ribbon drawing (made with MOLSCRIPT; Kraulis, 1993). The conserved water molecules are shown as white spheres and the d(CpA) inhibitor in black. The 3 helices are labeled H1, H2, and H3.

Borkakoti et al. (1982). The His 119 side chain occupies each position with an occupancy of approximately 0.5. In order to analyze the hydrogen bonding pattern associated with the B conformation, the absolute conformation of His 119 needs to be known. It is not possible to determine the absolute orientation of the imidazole from the electron density. It can be oriented in 2 different ways, related by a 180° rotation around the CB-CG bond. In the A conformation, the orientation of the imid-

Table 3. *Comparison of the hydrogen bonds in the active site of RNase A-inhibitor complexes*[a]

	3′-CMP		2′-CMP		d(CpA)		Sulfate	
Thr 43 O	O1′	3.5	O1′	3.5	–	–		
Thr 45 OG1	N3	2.9	N3	2.7	N3	2.8	–	
Thr 45 N	O2	2.7	O2	3.0	O2	3.0	–	
Wat	N4 (162)		N4 (147)		N4 (153)	3.1	–	
Wat	N4 (188)	3.1	N4 (219)	2.9	N4 (188)	3.3	–	
Wat	–		–		O5′ (169)	3.3	–	
Wat	O1′ (156)	3.2	O1′ (174)	3.0	O4′ (168)	3.4	–	
Gln 11 NE2	–		O2P	2.9	O2P	2.9	O4P	3.0
	Wat 157	2.8	Wat 170	3.1	Wat 138	3.0	Wat147	2.6
His 12 NE2	O2′	2.9	O1P	2.6	O1P	2.8	O1P	3.1
	O2P	2.7	–		–		O3P	2.8
Lys 41 NZ	O2′	2.7	O2′	3.3	–		–	
	Gln 11 OE1	3.1	Gln 11	3.2	–		–	
	Asn 44 OD1	2.7	Asn 44 OD1	2.8	Asn 44 OD1	2.6	Asn 44 OD1	2.6
His 119 ND1	O1P	3.2	O3P	2.5	O5′R	2.7	O2P	2.5
	O3P	3.1	–		O4′R	3.3	–	
Phe 120 N	O1P	2.7	O1P	2.9	O1P	3.1	O3P	2.8
Wat	O1P (185)	2.7	–		–		–	
Wat	O2P (157)	2.7	O1P (170)	3.1	O1P (138)	3.1	O3P (147)	2.5
	–		–		O2P (138)	3.2	–	
Wat	O3P (221)	2.8	–		–		–	
Asn 71 ND2	–		–		N1A	2.9	–	
Asn 71 OD1	–		–		N6A	2.8	–	
Wat	–		–		N6A (163)	3.2	–	
Wat	–		–		N7A (163)	2.7	–	

[a] X···A distances are given in Å. The sequence number of the water molecule of a particular structure involved in an interaction is given between parentheses and, in the d(CpA) complex atoms belonging to the ribose and adenine moieties of the downstream adenosine, are marked with an R and A, respectively.

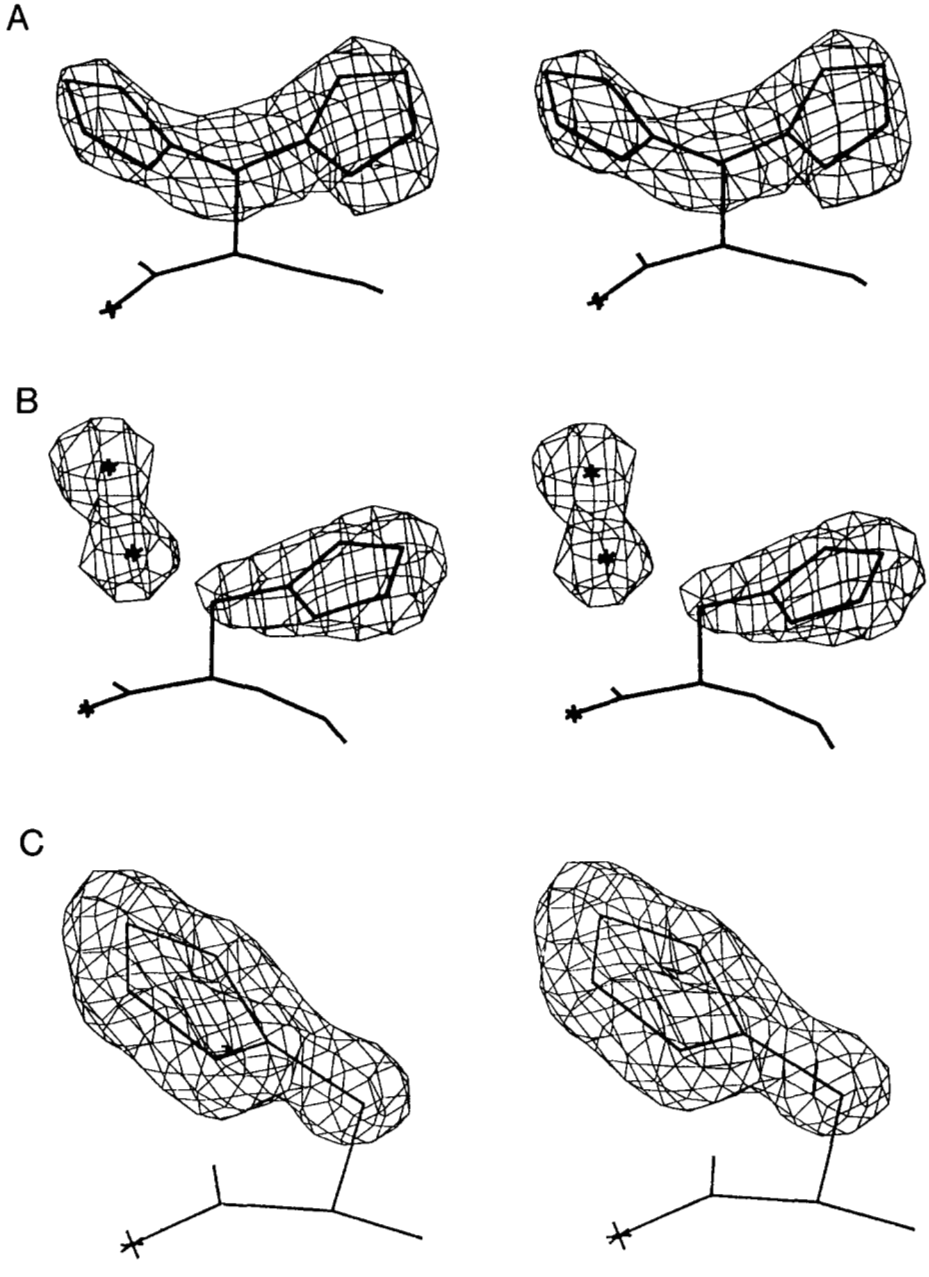

Fig. 3. Multiple conformations of His 119. $F_o - F_c$ difference density in the region of His 119 in (**A**) the native trigonal RNase A, (**B**) RNase A * 3′-CMP, and (**C**) RNase A * d(CpA). The pictures are taken from the same orientation. His 119 was removed from the coordinates and the structures refined for 9 cycles before the electron density was calculated.

azole has been determined by neutron diffraction studies (Wlodawer et al., 1983). If the A and B conformations were simply related by a rotation around the CA-CB bond, the His 119 would form a hydrogen bond with Wat 225 (119 ND1–225 O, 3.2 Å). A better hydrogen bonding network is obtained if the imidazole ring is flipped over by 180° around the CB-CG bond. The His 119 ND1 is now pointing toward the active site, forming a hydrogen bond with the 118 O, and Wat 225 is in van der Waals contact with the CD2 of His 119. This second orientation of His 119 was also the one observed in the NMR structure of RNase A (Santoro et al., 1993).

Interactions between RNase A and 3′-CMP

The 3′-CMP inhibitor is bound in an C2′-exo *anti* conformation (Table 3; see Kinemage 1), which is one of the energetically favorable conformations for nucleotides (Saenger, 1984). The *anti* conformation around the glycosidic bond confirms the interpretation of Karpeisky and Yakovlev (1977) of nuclear Overhauser effect studies of RNase A * 3′-CMP. The cytidine moiety forms 2 hydrogen bonds with Thr 45 and stacking interactions with Phe 120. The NH_2 group of the cytidine forms 2 hydrogen bonds with 2 water molecules, which, in their turn, interact with

Ser 123, Asp 83, and Thr 45. The ribose phosphate moiety is bound in the active site, making contact with all the active site residues. His 12 and Lys 41 form strong hydrogen bonds with the 2′-OH group of the ribose. Lys 41 further forms hydrogen bonds with Gln 11 and Asn 44 and is very clearly defined. His 119 takes up the B conformation (Fig. 3), which is relatively unusual for inhibitor complexes. In this conformation, His 119 still interacts with the phosphate but cannot form a hydrogen bond with Asp 121. The phosphate moiety of the 3′-CMP is further hydrogen bonded to His 12, the main chain of Phe 120, and to 3 water molecules. When the present structure is compared to the 2′-CMP complex of RNase A, it is clear that the cytidine and phosphate moieties of the inhibitors bind in very similar positions. The conformations of the riboses are slightly different, indicating that the ribose adapts itself to the phosphate and cytidine. The major differences are found in the interactions between the ribose-phosphate moiety and the active site: in the 2′-CMP complex there is only a weak interaction between the 2′ oxygen and Lys 41, His 12 only interacts with the phosphate, and Gln 11 forms a hydrogen bond with the phosphate.

Interactions of RNase A with d(CpA)

Figures 1 and 4 (Kinemage 1) show the d(CpA) bound to the active site of RNase A. It is bound in an extended conformation, with the cytidine in the specificity pocket, the phosphate in the active site, and the adenine in a subsite. Both deoxyriboses take up the energetically favorable C2′-exo *anti* conformation, similar to the 3′-CMP complex of RNase A (Table 3). The γ torsion around the C4′-C5′ bond of the adenosine is in the ap (antiperiplanar) range, and the α and ζ torsion angles around the phosphodiester bonds are both in the +sc (synclinal) range. These values are unusual for RNA in solution; there the γ torsion is mostly in the +sc range, which causes steric problems between the phosphates when the α and ζ torsion angles are both in the +sc range (Govil, 1976). In RNase A, however, the γ torsion angle is stabilized in the ap range by protein–inhibitor interactions. This seems to be a general feature of RNA and DNA chains bound to proteins (Saenger, 1984). A γ torsion angle in the ap range "opens up" the RNA chain, bringing the deoxyribose and phosphate in contact with the active site (Fig. 4). A second consequence of the γ torsion in the ap range is that there is no longer a problem with steric hindrance, and the phosphodiester bonds can take up +sc conformations that are otherwise forbidden. The +sc (and −sc) conformations are energetically favorable because the lone pairs on the O3′ and O5′ can donate electrons to the polarized P–O bonds of the phosphate oxygens (gauche effect; Srinivasan et al., 1980). The torsions around C5′–O5′ (β) and C3′–O3′ (ϵ) are, respectively, in the +ac (anticlinal) and the ap regions. The β torsion angle is relatively unusual for dinucleotides but not totally unprecedented (Saenger, 1984).

The cytidine base is bound in the specificity pocket in a similar way as in the 3′-CMP complex. It forms hydrogen bonds with main-chain and side-chain atoms of Thr 45, stacking interactions with Phe 120, and hydrogen bonds with 2 water molecules (Table 4). The deoxyribose belonging to the cytosine does not make any direct interactions with the protein and forms only 2 hydrogen bonds with water molecules. In the active site of the 3′-CMP complex, His 12 and Lys 41 interact with the 2′-OH, which is absent in d(CpA). In the d(CpA) complex, His 12 only forms a hydrogen bond with one of the phosphate oxygens, and Lys 41

Table 4. *Conformation of the 3′-CMP, 2′-CMP, and d(CpA) inhibitors, all bound to RNase A*

			d(CpA)	
	3′-CMP	2′-CMP	Cytidine	Adenine
Backbone torsion angles (deg)				
O5′-C5′-C4′-C3′ (γ)	−149	77	31	172
C5′-C4′-C3′-O3′ (δ)	82	57	122	139
C5′-C4′-C3′-C2′	−151	173	−115	−100
C4′-C3′-C2′-O2′	−121	−78	NR[a]	NR
C2′-C3′-O3′-P	73	100	81	NR
Glycosyl torsion angle (deg)				
O1′-C1′-N9-C4′ (χ)	−166 (anti)	−134 (anti)	−155 (anti)	−103 (anti)
Pseudorotation angles (deg)				
C4′-O1′-C1′-C2′ (ν_0)	18	1	−18	−24
O1′-C1′-C2′-C3′ (ν_1)	−28	−32	25	37
C1′-C2′-C3′-C4′ (ν_2)	27	48	−22	−35
C2′-C3′-C4′-O1′ (ν_3)	−16	−48	11	22
C3′-C4′-O1′-C1′ (ν_4)	−1	31	5	1
Phase	−20,5° C2′-exo	17,3° C3′-endo	−28,6° C2′-exo	−20.4° C2′-exo
Phosphodiester torsions angles of d(CpA) (deg)				
O3′-P-O5′-C5′ (α)	77			
P-O5′-C5′-C4′ (β)	110			
C4′-C3′-O3′-P (ϵ)	−160			
C3′-O3′-P-O5′ (ζ)	55			

[a] NR, not relevant.

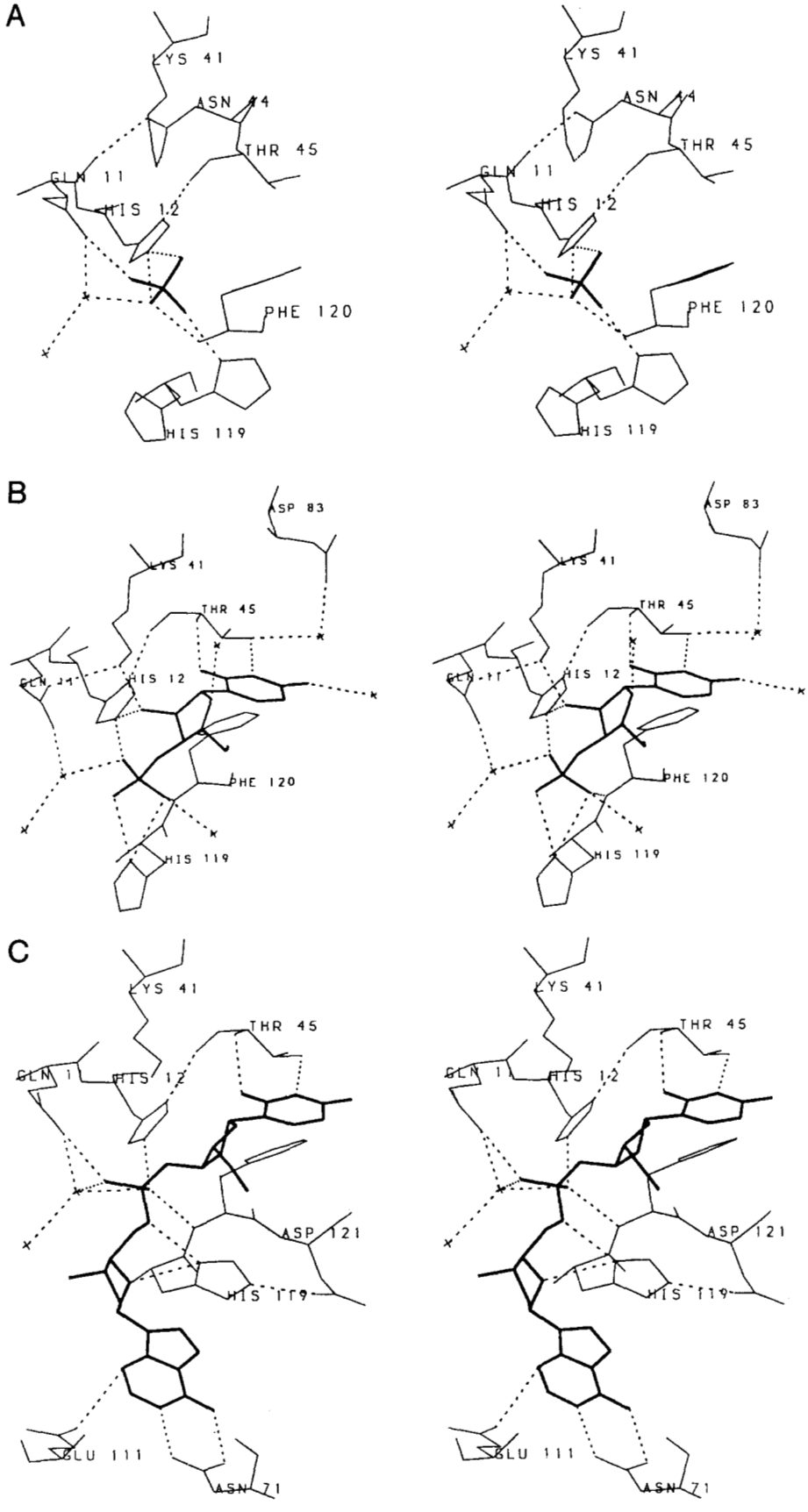

Fig. 4. Active site region is shown for the final structures of **(A)** the native trigonal RNase A, **(B)** RNase A * 3′-CMP, and **(C)** RNase A * d(CpA). The sulfate and the inhibitors are shown in bold and the hydrogen bonds as dashed lines.

has 2 conformations, in one of which it forms a hydrogen bond with Asn 44. Gln 11, the main-chain N of Phe 120, and a water molecule form hydrogen bonds with the phosphate oxygens. His 119 takes up the A conformation (Fig. 3). In this orientation His 119 interacts on one side with the leaving O5′ oxygen and the O4′ of the downstream deoxyribose, and on the other side with Asp 121. The downstream deoxyribose is not involved in any other interactions with the protein and is not as well defined as the deoxyribose of the cytosine. The downstream adenine is bound in an area, which is similar to the one previously observed in RNase A dinucleotide complexes discussed by Wlodawer (1984). The details of the interactions are, however, better defined and different from what was previously observed. In contrast to previous structures, the adenine only forms 2 strong hydrogen bonds with Asn 71 and 2 with water molecules, and none with Gln 69, Glu 111, or other residues. The adenine displaces 2 water molecules, which, in the native structure, take up positions similar to the N1 and N6 of the adenine, forming similar hydrogen bonds with Asn 71. The downstream adenine is further involved in stacking interactions with His 119, which is only possible when His 119 takes up the A conformation. Two residues in the neighborhood of the adenine, i.e., Gln 69 and Asn 67, have multiple conformations. In its low-occupancy conformation (occupancy 0.25), Gln 69 is in close contact with the adenine N6. In its second conformation (occupancy 0.75), Gln 69 is in close contact with the low-occupancy conformation of Asn 67. In its second conformation, Asn 67 avoids close contact with Gln 69. Apparently, when the adenine binds, Gln 69 and Asn 67 move away together. In their high-occupancy conformation, Asn 67 and Gln 69 do not interact with the adenine.

Geometry of the active site of RNase A compared to RNase T1

RNase T1 is the best known representative of a family of microbial ribonucleases, whose 3-dimensional structure was first determined by Heinemann and Saenger (1982). Structural and kinetic studies have shown that in RNase T1, His 40, Glu 58, and His 92 act as the electrostatic catalyst, the general base, and the general acid, respectively, in a concerted reaction (Osterman & Walz, 1978; Takahashi & Moore, 1982; Steyaert et al., 1990). RNase A and RNase T1 are not homologous either in sequence or in structure. They have both evolved, however, to catalyze the same reaction: both enzymes cleave the P-O5′ bond in RNA and hydrolyze the cyclic nucleotide that is formed in the first reaction. Nonaka and colleagues (1993) compared the geometry of the catalytic residues of a number of microbial RNases and RNase A. They found that the general acids and general bases superimpose. Comparison of the present 3′-CMP and d(CpA) complexes of RNase A with a structure of RNase T1 complexed with 3′-GMP and guanosine (Zegers et al., 1994) indicates which features of the active site are similar in the 2 ribonucleases and which features are more variable. RNase A can be superimposed on RNase T1 on the basis of the inhibitor atoms that are central in the catalyzed reaction, i.e., the atoms of the ribose-phosphate moieties of the inhibitors. Figure 5 shows the active sites of RNase A * 3′-CMP and RNase d(CpA) superimposed on RNase T1 * 3′-GMP + Guo. The specificities of RNase A and RNase T1 are different: RNase A cleaves RNA after pyrimidines and RNase T1 is specific for guanine. The structures of the enzymes reflect this. In RNase T1, the nucleotide in the major binding site is in a *syn* conformation, and in RNase A it is *anti*, and the cytidine (RNase A) and guanine (RNase T1) bases do not superimpose. The only similarity is that in both enzymes the bases are stacking with an aromatic side chain (Tyr 42 in RNase T1 and Phe 120 in RNase A). There are some remarkable similarities when the catalytic sites of the 3′-CMP and 3′-GMP complexes of, respectively, RNase A and RNase T1 are compared. The superposition of the 3′-CMP complex of RNase A on RNase T1 brings His 12, the general base of RNase A, very close to Glu 58, the general base of RNase T1. Furthermore, Lys 41 from RNase A comes close to His 40 of RNase T1. Although the nitrogens of the lysine and histidine do not fall in the same position, they can form a very similar hydrogen bond with the 2′ oxygen because of the different geometry of these nitrogens: in the histidine it is aromatic, whereas the lysine contains a primary nitrogen, with C-N-H angles of 106°. Thus, the structures of RNase A and RNase T1 have the same geometry as far as the 2′-OH group of the substrate analogues is concerned. The general acids, His 119 in RNase A and His 92 in RNase T1, superimpose well when the d(CpA) complex (with His 119 in the A conformation) of RNase A is compared to RNase T1. When the 3′-CMP complex (with His 119 in the B conformation) is compared, the general acids do not superimpose. Other residues that are in contact with the phosphate are more variable; the Gln 11 and a conserved water molecule in RNase A are in the same area as the catalytic residue Tyr 38 in RNase T1. The Phe 120 N of RNase A does not have a direct structural counterpart and neither has Arg 77 of RNase T1. These residues probably play a role in the electrostatic stabilization of negative charges on the phosphate oxygens, on which the stereochemical constraints may be smaller. The transesterification rates of RNase A and RNase T1 both vary with the nature of the leaving nucleoside N in XpN, although the nature of the downstream bases has little effect on the binding of dinucleotides (Witzel & Barnard, 1962; Steyaert et al., 1991). Both enzymes have a subsite in which the downstream base binds. When the d(CpA) complex of RNase A is superimposed on the 3′-GMP + Guo complex of RNase T1, we find that the position of the adenine in RNase A is very close to that of the guanine in RNase T1, even if the atoms of the bases in the subsites were not used for the superposition (Fig. 5).

Structurally conserved water molecules

In order to determine which water molecules are most closely associated with the protein we determined which water sites were conserved in 10 independently refined RNase A structures derived from 5 different crystal forms (Table 2). Williams et al. (1987) determined the structure of the glycosylated form of RNase B from a sixth crystal form C2, but they did not include water molecules in the refinement. The structures we used were determined at a resolution of at least 2.2 Å and were well refined. One crystal form contains 2 molecules per asymmetric unit (8RSA, Nachman et al., 1990). These 2 RNase A molecules have been treated independently, each time with all the water molecules of the asymmetric unit. Five of the RNase A structures are covalently modified. A water site associated with a region that is covalently modified in one of the structures was still considered conserved if it was absent only in the concerned modified structure. The modified structures are: RNase S (2RNS, Kim et al., 1992), where the peptide bond between Ala 20 and Ser 21 has been cleaved and residues 16–20 are not clearly de-

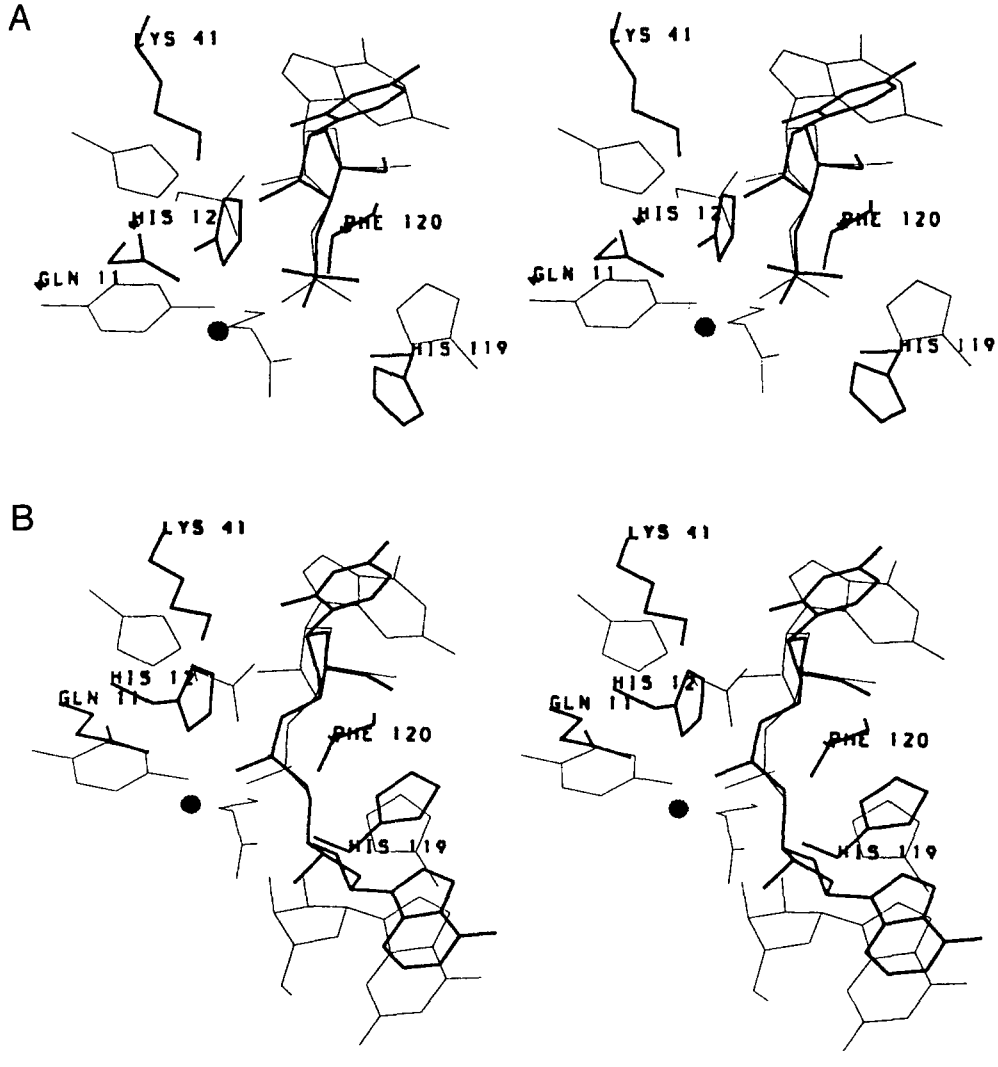

Fig. 5. Superposition of RNase A on RNase T1. The active site of RNase A (bold lines, Gln 11, His 12, Lys 41, His 119, Phe 120, and the inhibitor) was superimposed on the active site of RNase T1 (thin lines, Tyr 38, His 40, Glu 58, Arg 77, His 92, 3′-GMP, and guanosine) on the basis of the atoms of the ribose-phosphate moiety. **A:** RNase A * 3′-CMP superimposed on RNase T1*3′-GMP + Guo. **B:** RNase A * d(CpA) superimposed on RNase T1*3′-GMP + Guo. Only the residues of RNase A are labeled.

fined in electron density; a structure with Lys 7 crosslinked to Lys 41 (1RSM, Weber et al., 1985); the semisynthetic complex of residues 1–118 with residues 111–124 (4SRN, Martin et al., 1987); and the 2 structures in the asymmetric unit of the RNase A T * H12 (8RSA, Nachman et al., 1990), where a thymidine was covalently bound to His 12. The modification in this last structure has only a limited effect on the structure of the protein. The numbers of the conserved water sites cited further in the text correspond to the numbers of the water molecules in the d(CpA) complex of RNase A.

In Table 5, the different RNase A structures are compared pairwise. The number of water molecules conserved in pairs of structures varies from 20 to 102, for RMS deviations between the backbone atoms of pairs of structures that vary between 0.16 and 0.79 Å. There is no structure that is a clear outlier, indicating that the water shells of the different structures can indeed be compared. When structures within the space group $P2_1$ are compared (7RSA, 1ROB, and d(CpA)), 35 conserved water sites are found and, within the space group $P3_221$ (1RPH, 1RPF, and 4SRN), 32 water sites are conserved. When all water sites of structures from those 2 space groups are compared, 19 water sites are identical, which is only slightly higher than the 17 sites that were conserved in structures from all 5 space groups (Fig. 6; Table 6). Most water sites that are conserved within structures from one space group, but not in structures from different space groups, are involved in direct packing contacts or in water networks that relate symmetry-equivalent molecules. Two of the conserved sites (129, 144) are absent in RNase S (2RNS) because they are associated with the region that is covalently modified. Similarly, sites 139 and 133 are absent in the semisynthetic structure 4SRN, and site 137 in the crosslinked structure 1RSM. The 17 conserved water molecules all form direct hydrogen bonds to the protein and are thus part of the first hydration shell. The average temperature factor of the conserved water molecules of the d(CpA) complex is 20.8 $Å^2$, as compared to 40.6 $Å^2$ for all water molecules, and 15.7 $Å^2$ for all

Table 5. *RMS differences between different RNase A structures*[a]

	1RPG	2CMP	7RSA	1RPH	1RPF	4SRN	1RSM	8RSA1	8RSA2	2RNS
1RPG	–	77	102	39	47	36	36	40	42	36
2CMP	0.16	–	71	29	38	28	27	33	38	27
7RSA	0.17	0.26	–	44	46	49	43	52	53	49
TRIG	0.37	0.44	0.41	–	50	45	22	34	33	30
3CMP	0.40	0.47	0.49	0.34	–	37	23	46	35	32
4SRN	0.63	0.71	0.66	0.56	0.63	–	28	38	41	30
1RSM	0.47	0.52	0.45	0.58	0.66	0.78	–	21	23	20
8RSA1	0.51	0.59	0.54	0.48	0.49	0.69	0.67	–	57	32
8RSA2	0.54	0.61	0.54	0.48	0.53	0.64	0.67	0.29	–	28
2RNS	0.65	0.69	0.66	0.55	0.55	0.67	0.79	0.65	0.63	–

[a] The upper half of the table contains the number of water molecules that are conserved in pairs of structures. The lower half contains the RMS differences (Å) between the backbone atoms of the 2 structures after the structures have been superimposed by least-squares refinement. The structures are identified by the Brookhaven code or an abbreviation (present structures) and are listed in Table 2.

protein atoms. Most of the conserved sites are found in small clusters of 2 and 3 and are part of extended networks of water molecules that are more variable in position. None of these water molecules is completely buried within the protein.

Of the 17 conserved sites, 13 are directly or indirectly associated with one of the 3 helices of RNase A. Three clusters of, respectively, 2, 2, and 3 water sites are associated with the N-terminal α-helix and link the helix to the C-terminal β-strands. The first cluster consists of waters 137 and 138, which are associated with the active site (Fig. 6A; Kinemage 1). Sekharudu and Sundaralingam (1993) classified the water molecules that are associated with helices as internal (hydrogen bonded to both $C{=}O_i$ and N_{i+4}) or external (hydrogen bonded to only $C{=}O_i$). Water 137 is bound to the N-terminal helix as an external water: it makes a hydrogen bond to the O4 while the hydrogen bond between the O4 and N8 is still intact. On the other side, water 137 forms a hydrogen bond with O118 and with Wat 138. Wat 138 is remarkable because it always interacts with the inhibitors in RNase A * inhibitor complexes. It forms hydrogen bonds to Gln 11, sometimes to His 12, and always to the phosphate or sulfate group in the active site; it is an integral part of the active site. The second cluster consists of Wat 131 and 135 and links the N-terminal helix to the C-terminal β-strand and H3. Wat 131 is, similar to Wat 137, an external water forming a hydrogen bond with O5 of the helix. The third cluster, sites 132, 139, and 133, link the beginning of the N-terminal helix to the β-pleated sheet. Wat 132 is hydrogen bonded to N5, which is at the end of the N-terminal helix.

The second helix of RNase A (residues 24–34) contains 1 conserved internal water site (Wat 129, Fig. 6B; Kinemage 1) at the start of the helix, forming hydrogen bonds with O23 and N27, which are 5.3 Å apart. Wat 129 and 134 further link the start

Table 6. *Hydrogen bonds of the conserved water molecules*[a]

Water[b]	Hydrogen bonds									
128	52N	3.0								
129	23O	2.6	97O	2.9	27N	3.0	99OG1	3.0	W242	3.5
130	83OD2	3.2	98O	3.0	83O	3.1	100OG1	2.7	W274	3.0
131	117O	2.8	5O	3.0	W135	2.5				
132	5N	3.1	4N	3.5	W139	2.8	W186	3.2		
133	114O	2.9	W139	2.9						
134	23O	3.0	99N	2.9	W158	3.1				
135	55NE2	2.9	9OE2	3.1	W131	2.5				
136	53O	2.7	60NE2	3.0	W201	2.9	W140	3.4		
137	118O	2.7	4O	2.8	W138	3.0				
138	126O1P	3.1	126O2P	3.1	11NE2	3.0	W137	3.0		
139	111O	3.0	W132	2.8	W133	2.9				
140	77N	3.0	77OG	2.7	60OE1	2.8	76N	3.2	W201	3.3
141	62N	3.2								
142	50N	2.9	49OE2	2.6	53OD2	2.7				
143	101N	3.1	W264	2.9						
144	18OG	3.3	18N	3.5	W267	3.0				

[a] The distances for the hydrogen bonds in which the conserved water molecules take part are given in Å and are taken from the d(CpA) complex of RNase A.

[b] The numbers correspond to the residue numbers of the conserved water molecules in the d(CpA) complex of RNase A.

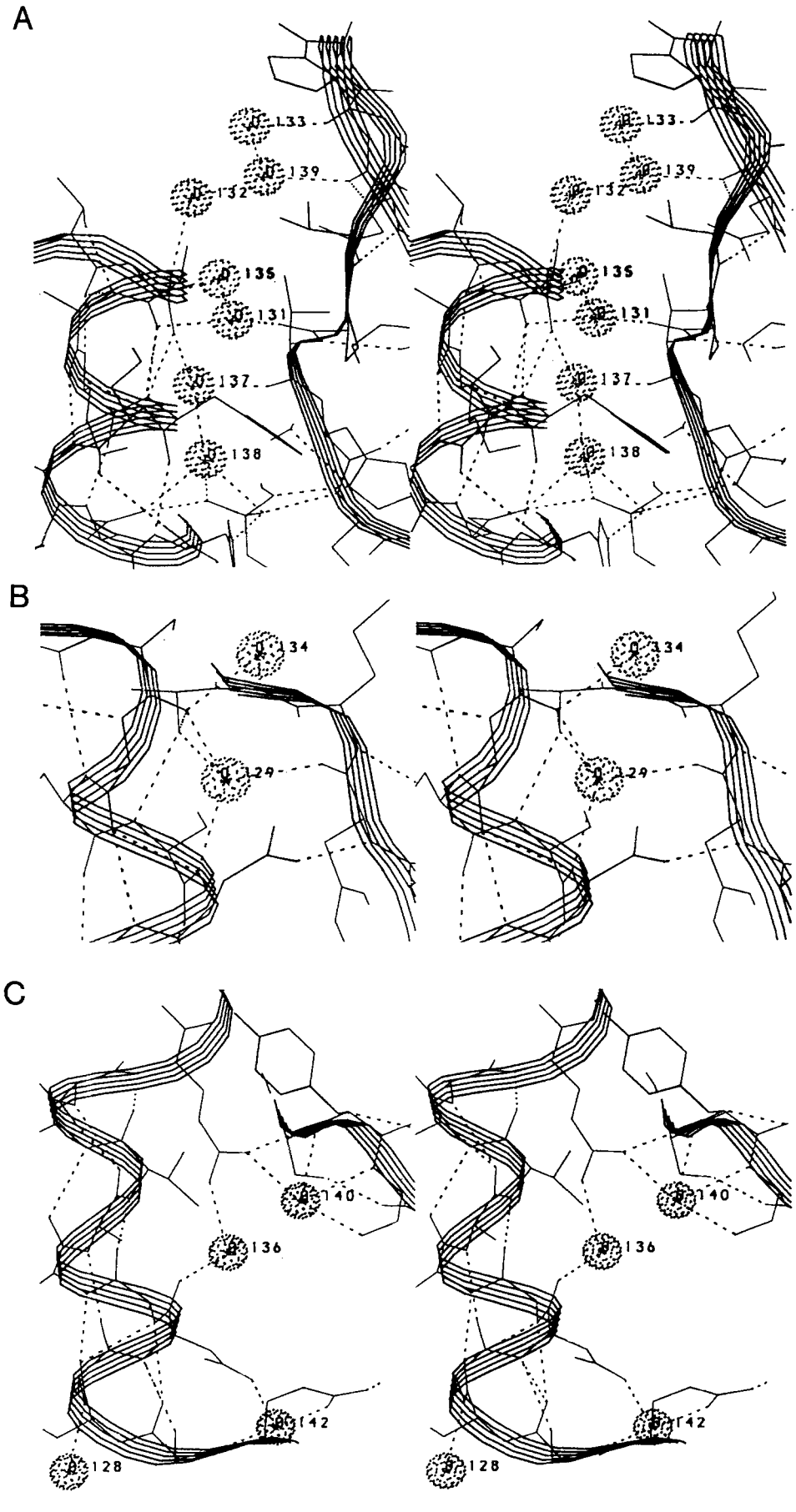

Fig. 6. Conserved water molecules in the helices. The conserved water molecules are often associated with helices. **A:** Conserved water molecules associated with the N-terminal helix. **B:** Internal water molecule at the start of the second helix. **C:** Water molecule 136 associated with the change from an α-helix to a 3_{10}-helix in the third helix of RNase A.

of the second helix to the β-sheet, initiating the contact between the 2 secondary structure elements.

The third helix of RNase A (residues 50–60) is strongly distorted; residues 50–55 form a partially distorted α-helix, whereas residues 56–60 distort further toward a 3_{10}-helix. Three conserved water sites are directly associated with this helix (142, 128, and 136), and 1 other water site (140) is linked to Wat 136 (Fig. 6C; Kinemage 1). The start of the helix is stabilized by Wat 142, which links the OG1 50 and N50 to OD2 53. Wat 128 saturates the free main-chain nitrogen of residue 52 at the N-terminus of the helix. Wat 136 is an external water hydrogen bonded to the main-chain carbonyl of residue 53 (Fig. 6C; Kinemage 1). This interaction compensates for the absence of the O53–N57 hydrogen bond (3.9 Å) expected in an α-helical segment. The next carbonyl in the helix (residue 54) forms a weak hydrogen bond with N57 (3.4 Å) and none with N58 (4.5 Å). The following hydrogen bonds of the helix are $C{=}O_i \cdots N_{i+3}$ bonds characteristic of a 3_{10}-helix. Wat 136 further forms a hydrogen bond to the conserved Wat 140, which in its turn is hydrogen bonded to side chains of β-sheet.

Four conserved water sites are not in contact with the helices. Three of those (144, 141, and 143) saturate free N-H and C=O groups on the surface of the protein. The last conserved water molecule (130) is found on top of the β-pleated sheet, forming hydrogen bonds with the N98 and O83 and with the side chains of Thr 100 and Asp 83. The interaction with Asp 83 might be important for the binding of pyrimidines, because Asp 83 is, in its turn, hydrogen bonded to a water molecule that is part of the specificity pocket in all the structures that contain a pyrimidine in the major binding site.

Discussion

We present 3 structures of RNase A: a native structure (with a sulfate in the active site), a 3′-CMP complex (both determined from trigonal crystals), and a d(CpA) complex determined from monoclinic crystals (Kinemage 1). Neither the binding of the 3′-CMP or d(CpA) inhibitors nor the change in space group caused any major differences in the conformation of the protein.

The structure of RNase A complexed with d(CpA) was primarily determined in order to gain more detailed information on the interactions at the downstream binding site and to compare the binding mode to that found in the crystal structures of RNase A soaked with 2′,5′-CpG and d(CpG) (Aguilar et al., 1991, 1992). In those last 2 high-resolution structures, the downstream guanine was bound in the major binding site, and the active site was occupied by an inorganic sulfate or phosphate anion. This binding mode was dubbed retro-binding. Because the retro-binding was also observed in co-crystals of RNase A with d(CpG) (Lisgarten et al., 1994), this binding mode could not be due to the soaking procedure employed. Early work on crystal structures of RNase A complexed with dinucleotides (UpcA, Richards & Wyckoff, 1973; 2′,5′-CpA, Wodak et al., 1977; 2′F-dUpA, Pavlovsky et al., 1978) showed that the dinucleotides with a downstream adenine were "properly" bound. Because these structures were determined at low resolution and often not refined, some questions on the precise mode of binding of downstream bases remained. The present structure shows that, in contrast to the 2′,5′-CpG and d(CpG) molecules, the d(CpA) dinucleotide is bound in the active site, with the cytidine in the pyrimidine binding site and the adenine in a subsite. This confirms the early structures as well as the fact that the retro-binding occurs because of specific interactions between the guanine and the residues of the major binding site.

Implications for the mechanism of action

RNase A catalyzes the depolymerization of RNA through a transesterification reaction, which results in the cleavage of the P-O5′ bond at the 3′ end of pyrimidines. This reaction can be followed by the hydrolysis of the 2′,3′ cyclic nucleotide formed in the first reaction. Neither 3′-CMP nor d(CpA) are the real substrate or transition state of the reaction. The interpretation of the structures in terms of the catalytic mechanism is only possible by extrapolating from the protein–inhibitor interactions to protein–substrate or transition-state interactions. The 3′-CMP inhibitor in the present complex has, more than a 2′-CMP inhibitor, features in common with the substrate of the transesterification reaction. The ribose carries a phosphate group on the 3′ carbon, and a free 2′-OH on the 2′ carbon, and is thus very similar to the ribose in natural RNA. The d(CpA) inhibitor lacks the 2′-OH group that is essential for the reaction but is otherwise identical to a dinucleotide substrate of the transesterification reaction. Thus, the interactions between RNase A and the 3′-CMP and d(CpA) inhibitors can provide a reasonable interpretation in terms of the mechanism of action of the enzyme (Fig. 7).

Pyrimidine binding site

RNase A is specific for pyrimidines. This specificity is mainly achieved by hydrogen bonds from the ambivalent Thr 45, which can accommodate both uridine and cytidine, and by stacking interactions with Phe 120. These interactions were also systematically observed in previous protein–inhibitor structures (see Wlodawer, 1984). Additionally, the cytidine NH2 group interacts with 2 water molecules that link the cytidine to Asp 83 and Ser 123. One of those water molecules is also present in the native structure of RNase A. The 2 water molecules are not only conserved in the 3′-CMP and d(CpA) complexes presented here, but also in the 2′-CMP complex (Lisgarten et al., 1993) and the uridine vanadate complex determined by Wlodawer et al. (1983). These water molecules have been described by Gilliland et al. (1994) as forming an integral part of the binding site. The interactions through water molecules are perhaps more labile than through direct hydrogen bonds, but the fact that less water molecules need to be stripped from the protein and substrate is favorable. Moreover, the water molecules are very versatile; they can form hydrogen bonds to both the NH2 group of cytidine and the C=O group of uridine. The double substrate specificity for cytidine and uridine is thus achieved through the ambivalent hydrogen bonding characteristics of Thr 45 and of 2 water molecules.

Catalytic site

RNase A catalyzes the cleavage of RNA through a concerted general base–general acid mechanism (Findlay et al., 1962; Usher, 1969). It is generally assumed that His 12 acts as a general base, abstracting a proton from the 2′ oxygen of the ribose. The nucleophilic 2′ oxygen can then attack the phosphorus, forming a pentacovalent transition state with the 2′ and 5′ oxygens in the axial positions. The transition state carries 2 nega-

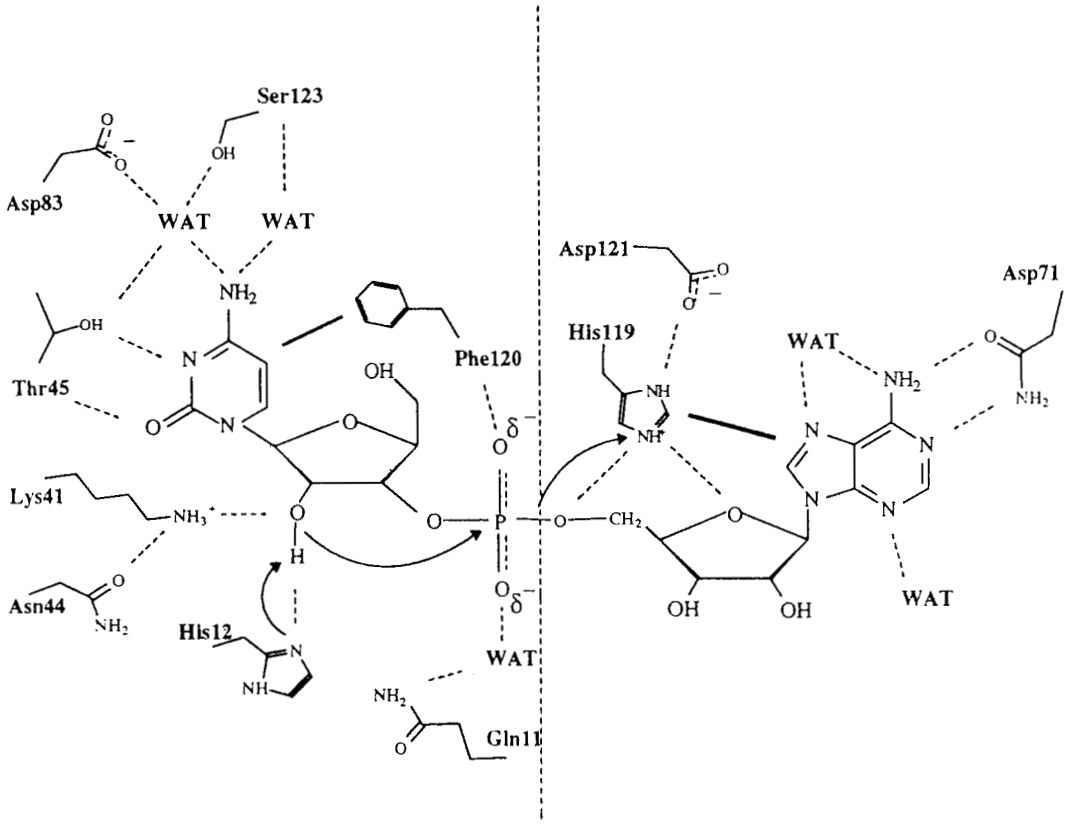

Fig. 7. Proposal for the RNase A–substrate interactions. Summary of the protein–inhibitor interactions in the active site of RNase A, and proposal for the protein–substrate interactions. Hydrogen bonds (shown as dashed lines) on the left of the central dashed line correspond to the interactions in the 3′-CMP complex of RNase A. Interactions in the subsite, on the right of the dashed line, are those from the d(CpA) complex of RNase A. Stacking interactions are indicated by a broad line. Movement of the electrons during the reaction is shown by arrows.

tive charges, as compared to 1 in the ground state. The general acid His 119 should be situated on the opposite side of the phosphate, protonating the 5′ leaving group. Lys 41 is essential for activity of the enzyme, as chemical modification studies (reviewed in Blackburn & Moore, 1982) and mutagenesis studies (Trautwein et al., 1991) have shown. It is thought to act as an electrostatic catalyst stabilizing the second negative charge formed in the transition state. The 3′-CMP complex permits the analysis of the interactions with the crucial 2′-OH moiety. The 2′-OH forms 2 strong hydrogen bonds, with His 12 and Lys 41. The strong hydrogen bond with His 12, which was not previously observed in RNase A inhibitor complexes, is in agreement with the view that His 12 acts as the general base, abstracting a proton from the 2′-OH group. The hydrogen bond between the 2′-OH and Lys 41 is perhaps more surprising. It was, in general, assumed that Lys 41 is involved in the stabilization of negative charges on the equatorial oxygens of the pentacovalent transition state (Roberts et al., 1969, Gerlt & Gassman, 1993). The present structures indicate that Lys 41 interacts directly with the 2′ oxygen. It seems a more general feature of ribonucleases that the electrostatic catalyst interacts with the 2′ oxygen of inhibitors because a similar hydrogen bond is found in the complex of RNase T1 with 3′-GMP (Heydenreich et al., 1993; Zegers et al., 1994). Davis and colleagues (1988) described the charge distribution of the base-catalyzed hydrolysis of aryl uridine-3′-phosphates and concluded that, in the transition state, there is a charge development on the attacking, 2′ oxygen. The electrostatic catalyst (Lys 41 in RNase A and His 40 in RNase T1) could stabilize this negative charge on the 2′ oxygen and thereby activate the substrate, facilitate the abstraction of a proton from the 2′-OH, and stabilize the transition state.

The conformation of His 119, which acts as the general acid during catalysis, has been the subject of some debate. Wyckoff et al. (1970) observed considerable motion of the imidazole side chain. Borkakoti et al. (1982) observed 2 conformations of the His 119 side chain (A and B) in RNase A crystallized from organic solvents. The present native structure of RNase A shows that these 2 conformations can also be found in high salt crystal forms of RNase A, and Santoro et al. (1993) describe the same 2 conformations of His 119 in NMR solution studies of RNase A. Wlodawer et al. (1982, 1983) observed only the A conformation, whereas 3 other groups observed only the B conformation (Martin et al., 1987; Nachman et al., 1990; deMel et al., 1992). In inhibitor complexes of RNase A, His 119 always has a single conformation, which can either be the A (O8-2′-CMP, Borkakoti, 1983; uridine vanadate, Wlodawer et al., 1983; 2′-CMP, Lisgarten et al., 1993) or the B conformation (O3-2′-CMP, Borkakoti, 1983). In the present 3′-CMP complex, the His 119 imidazole is present only in the B conformation, and in the d(CpA) complex, it takes up the A conformation (Kine-

mage 1). It appears that, in the absence of a substrate or inhibitor, His 119 is relatively mobile and has 2 preferential conformations, A and B. The binding of an inhibitor stabilizes the imidazole in 1 of the 2 preferential conformations. Borkakoti et al. (1982) proposed that the 2 conformations of His 119 reflect the fact that His 119 functions in 2 different reactions, i.e., the transesterification and the hydrolysis reactions. deMel et al. (1992) proposed that His 119 is active in position B during the transphosphorylation reaction and in position A during the hydrolysis reaction. The present structures, however, do not sustain this last proposal. The d(CpA) closely resembles a dinucleotide substrate of the transesterification reaction, at least as far as leaving O5′ group is concerned. In the structure of this complex, His 119 is in the A conformation and forms a hydrogen bond with the O5′ oxygen it should protonate in a real substrate. Additionally, when the active sites of RNase A and RNase T1 are superimposed, it is the A conformation of His 119 that superimposes on His 92, the general acid of RNase T1. It seems most probable that His 119 is active in the A conformation during the transesterification reaction.

In conclusion, the transesterification reaction is catalyzed by the general base His 12 and the electrostatic catalyst Lys 41, which interact with the 2′-OH, and the general acid His 119, which takes up the A conformation and interacts with the 5′ oxygen. The orientation and position of the 3 equivalent residues in RNase T1 (Glu 58, His 40, and His 92) are very similar to those in RNase A. The reaction can further be catalyzed by the stabilization of negative charges of the phosphate oxygens by Gln 11, the main-chain N of Phe 120, and a water molecule (Wat 138 in the d(CpA) complex), which is strictly conserved in all RNase A structures.

Downstream binding

RNase A catalyzes the cleavage of NpX nucleotides with a preference for X = A > G > C > U (Witzel & Barnard, 1962; Tarragona-Fiol et al., 1993). In previously determined dinucleotide complexes of RNase A, the subsite seems to be formed by Glu 69, Asn 71, Glu 111, and His 119. The present d(CpA) complex permits a detailed analysis of the interactions in the subsite. The adenine is stacked onto the general acid His 119 and forms 2 parallel hydrogen bonds with Asn 71. This is a very stable arrangement and is frequently found in protein–adenine interactions (Saenger, 1984). It is possible that Asn 71 can form similar hydrogen bonds with cytosine and also with guanine and uridine when the OD1 and ND2 of Asn 71 are inverted. Glu 69 and Asn 67 move away from the subsite in a concerted way, and Glu 111 does not interact with the adenine. Tarragona-Fiol et al. (1993) mutated the residues that were thought to be involved in the binding of the downstream base, i.e., Gln 69, Asn 71, and Glu 111. They found that the mutation of Gln 69 and Glu 111 only has a limited effect on the rate of transesterification of dinucleotides. On the other hand, the Asn 71 Ala mutation lowers the transesterification rate considerably. The protein–inhibitor interactions in the downstream binding site of the d(CpA) complex confirm their results and provide a structural basis for understanding the effect of the mutations. The binding of the downstream base has a major influence on the torsion angles of the ribose-phosphate backbone of the substrate. The protein–adenine interactions stabilize the "open" conformation of the dinucleotide. In this conformation, the phosphoribose moiety is accessible for the active site residues, and the 5′ leaving oxygen is strongly exposed to the general acid His 119. The fact that in RNase T1 the downstream base binds in a very similar position with respect to the active site confirms that the geometry of the downstream binding site is, together with that of the major active site residues, determined by the stereoelectronic restraints of the reaction.

Conserved water sites

The presence of water is essential for protein folding, stability, and activity. In X-ray structures of RNase A, 100–200 water molecules can be identified. Close to the protein, one observes the electron density for clearly defined solvent sites. Further from the surface, the electron density evolves into a continuum. This corresponds to a gradual change from individual water molecules, each with its specific environment, to water with bulk properties. Wlodawer et al. (1986) compared 2 independently refined structures of RNase A and found that most water molecules were conserved. The present study looked at water sites that are strictly conserved; only those sites where the water molecules of 10 different structures fell within a sphere of 0.5 Å radius after superposition of the structures were retained. This means that the positions of the conserved water molecules show a scatter similar to that of the backbone atoms (RMS deviation 0.2–0.8 Å). The present study shows that, although a large number of water molecules is not conserved according to the criteria used, a set of conserved water molecules, inherent to the structure of RNase A, has been identified (see Kinemage 1). Such sets of "structural" water molecules were previously observed for RNase T1 (Malin et al., 1991; Pletinckx et al., 1994), and for legume lectins (Loris et al., 1994), and seem to be a general feature of protein structures.

The structural importance of the conserved water molecules is clear from their position with respect to the secondary structure elements of the protein. Most conserved water molecules are associated with the helices of RNase A and link them to the β-sheets. In some cases, they are integral parts of the helices. Conserved water molecules are involved in the initiation of the second and the third helix, they stabilize the distortion from an α-helix to a 3_{10}-helix in the third helix, and link the N-terminal helix to the rest of the protein.

It is remarkable that all 7 water molecules associated with the N-terminal helix are also conserved in RNase S, where the helix is not covalently linked to the rest of the protein and can dissociate reversibly from the rest of the protein (Richards & Vithayathil, 1959). The hydrophobic residues in the C-terminal part of this helix that are involved in the reassociation with the rest of the protein have been studied (Varadarajan et al., 1992). The crystal structures show, however, that hydrogen bonds, direct or water-mediated, also play a role in the association of the helix. On one side, the N-terminal helix is linked to the second helix by an extended network of hydrogen bonds in which Arg 10 and Arg 33 play a central role. Arginines can span large distances and form many hydrogen bonds with residues that are situated relatively far from each other. Therefore, they can link several secondary structure elements together. On the other side of the helix, which is facing toward the active site and the C-terminal β-strands of RNase A, we do not find any direct contacts via side chains. Instead, a number of water molecules fill the space between the helix and the C-terminal β-

strands. All 7 conserved water molecules that are associated with the N-terminal helix are found in this region. One role of those water molecules clearly resides in the stabilization of the active site: they link the N-terminal helix, which carries the active site residues Gln 11 and His 12, with the C-terminal β-strand, with residues His 119 and Phe 120. Secondly, the fact that it is precisely on this side of the helix that water molecules are involved in the association of the helix with the rest of the protein indicates that they could be important for catalysis. Meyer (1992) proposed that chains of water molecules function as a "proton wire," bringing the active site in contact with the bulk water. The conserved waters could be part of such a proton wire. Indeed, one of the conserved water sites is directly associated with the phosphate of the inhibitors and is present in all the structures despite the large variation of inhibitors present in the active site.

The question of the significance of the other water molecules identified by X-ray crystallography remains. These water molecules are often conserved in some of the structures, even if those structures were refined independently. This indicates that they do correspond to a physical reality. The partially conserved water sites seem to correspond to preferred hydration sites that have the correct hydrogen bonding characteristics for accepting water molecules but where the presence of a water molecule is not essential for the structure of the protein. Most of these water sites are part of larger water networks that could represent different solvent environments present in solution. The fact that more water molecules are conserved within one spacegroup indicates that the packing and crystallization conditions "freeze out" some of the solution networks.

Finally, the 2 water molecules present in the binding site should be mentioned. Although they are not conserved in all structures of RNase A, they are present in all structures where a pyrimidine is bound. These 2 water molecules are an integral part of the binding site and can form hydrogen bonds both to cytidine and uridine. They form an example of how a protein can make use of the characteristics of water molecules and combine stabilization with versatility.

Materials and methods

Crystallization and data collection

RNase A (Sigma, type XIIA) was purchased from Sigma. Trigonal crystals of the native enzyme were obtained by the hanging drop vapor diffusion method. A solution containing 35 mg/mL protein in 20 mM sodium phosphate, 20 mM sodium acetate, pH 6, was equilibrated against 35% ammonium sulfate, 1.5 M sodium chlorine. Crystals of $1 \times 1 \times 1$ mm^3 grew after 1 week and were of space group $P3_221$. Crystals of the 3′-CMP complex of RNase A were obtained by soaking native crystals in mother liquor to which 3′-CMP was added at a final concentration of 10 mM for 24 h. The monoclinic d(CpA) complex of RNase A was crystallized in sitting drop setups. A solution containing 35 mg/mL protein and 10 mM d(CpA) in 20 mM phosphate, 20 mM acetate, pH 5.2, was equilibrated against 50% MPD.

Details about data collection are listed in Table 1. Data on the trigonal crystals were collected on a MAR Image Plate mounted on a rotating anode generator operated at 40 kV, 70 mA, with a Ni filter, and a 0.3-mm collimator. The crystal-to-screen distance was 100 mm. Data were collected at 2°/frame with an exposure of 30 min/frame. The native crystal was mounted with the *c*-axis along the oscillation axis, and 15 frames (30°) were collected. The crystal of the 3′-CMP complex was mounted in a random orientation, and 47 frames (94°) were collected. The data were processed with MOSFLM and other programs from the CCP4 package (Collaborative Computer Project 4, SERC Daresbury Laboratory, UK). The statistics are listed in Table 1. The data on the monoclinic d(CpA) complex were collected on an Enraf Nonius FAST Area detector mounted on a rotating anode operated at 45 kV and 50 or 70 mA. Data were collected at 22 or 60 s/frame, at 0.12°/frame. The shorter data collection times and lower amperages were used in order to collect the low-resolution data. The data reduction was performed with the program MADNESS (Messerschmidt & Pflugrath, 1987).

Structure determination

Trigonal crystals

The molecular replacement for the native data set was performed with the structure of the 2′-CMP complex of RNase A (Lisgarten et al., 1993) as a model. The orientation of the molecule in the unit cell was determined with the Crowther rotation function (Crowther, 1967) as implemented in the program MERLOT (Fitzgerald, 1988). The model was positioned in a P1 cell with 60-Å edges and transformed to produce structure factors from 4 to 10 Å. A Patterson map with a sphere of 15 Å was calculated and searched for peaks over 2.5° increments. A major peak was found with 4.6σ above background and refined by a 0.5° grid search. The molecule was positioned within the cell by using the translation function of the program TFSGEN (CCP4). In the spacegroup $P3_221$, a clear peak was found at 12σ above background. This solution is the same as the one previously found for a semisynthetic complex of residues 1–118 with 111–124 (Martin et al., 1987). The native trigonal structure was used as a model for the 3′-CMP complex.

Monoclinic d(CpA) complex

The isomorphous 2′-CMP complex of RNase A (Lisgarten et al., 1993) was used as a model, and the position in the unit cell was refined by rigid body refinement with the program RESTRAIN (Haneef et al., 1985).

The 3 structures were refined with a similar procedure using the program RESTRAIN (Haneef et al., 1985). All nonprotein atoms were deleted from the original coordinate file. After convergence of an initial rigid body refinement, the positions were refined for 10 cycles with an overall temperature factor and with individual temperature factors until convergence. The refinement was alternated with manual model revisions with the program FRODO (Jones, 1985) on an Evans and Sutherland PS390. Water molecules were inserted in sites that had a spherical difference density that was larger than 3σ in the $F_o - F_c$ map and showed a reasonable hydrogen bonding geometry. After refinement, it was checked if the water molecules were positioned in a peak higher than 1σ in the $2F_o - F_c$ map. Water molecules with high temperature factors were retained if they showed sufficient electron density. Regions with poor electron density were deleted from the model and rebuilt after refinement. The 3′-CMP and d(CpA) inhibitors were built into the electron density after the restrained refinement with individual temperature factors had converged. The occupancies of multiple conforma-

tions were initially given a value of 0.5 and refined during subsequent stages of the refinement.

Structure interpretation

Criteria that were used in assigning hydrogen bonds were: donor-acceptor distance cutoff at 3.5 Å and D-H···A angle larger than 90°. Structures were compared after a superposition based on the least-squares superposition of the backbone atoms. Conserved water sites were identified with the program FIXWAT (Lisgarten et al., 1993), which superimposes 2 structures, generates symmetry-equivalent water molecules, and checks which waters are closer than a limiting value. Water sites were considered conserved if the waters of all the different structures fell within a sphere of radius 0.5 Å after superposition of the structures. The structures of RNase A were superimposed on that of RNase T1 * 3′-GMP + Guo (Zegers et al., 1994) on the basis of the atoms of the ribose-phosphate moiety of the nucleotides. The C1′, C2′, C3′, C4′, C5′, O4′, O2′ (if present), O3′, and P of the 3′-CMP or d(CpA) inhibitors of RNase A were superimposed on the C1′, C2′, C3′, C4′, C5′, O4′, O2′, O3′, and P of the 3′-GMP in RNase T1.

Acknowledgments

This work was supported by the Vlaams Actieprogramma Biotechnologie and the EEC (Bridge grant). We thank Philip Stas for the calculation of the solvent accessibility of conserved water molecules and Maria Vanderveken for excellent technical assistance.

References

Aguilar CF, Thomas PJ, Mills A, Moss DS, Palmer RA. 1992. Newly observed binding mode in pancreatic ribonuclease. *J Mol Biol 224*:265–267.

Aguilar CF, Thomas PJ, Moss DS, Mills A, Palmer RA. 1991. Novel non-productively bound ribonuclease inhibitor complexes – High resolution X-ray refinement studies on the binding of RNase-A to cytidylyl-2′,5′-guanosine (2′,5′CpG) and deoxycytidylyl-3′,5′-guanosine (3′,5′dCpdG). *Biochim Biophys Acta 1118*:6–20.

Beintema JJ, Schuller C, Irie M, Carsana A. 1988. Molecular evolution of the ribonuclease superfamily. *Prog Biophys Mol Biol 51*:165–192.

Blackburn P, Moore S. 1982. Pancreatic ribonuclease. In: Boyer PD, ed. *The enzymes*. New York: Academic Press. p 317–433.

Borkakoti N. 1983. The active site of ribonuclease A from the crystallographic studies of ribonuclease-A-inhibitor complexes. *Eur J Biochem 132*:89–94.

Borkakoti N, Moss DA, Palmer RA. 1982. Ribonuclease A: Least squares refinement of structure at 1.45 Å resolution. *Acta Crystallogr B 38*:2210–2217.

Crestfield AM, Stein WH, Moore S. 1963. Alkylation and identification of the histidine residues at the active site of ribonuclease. *J Biol Chem 238*:2413–2420.

Crosio MP, Janin J, Jullien M. 1992. Crystal packing in six crystal forms of pancreatic ribonuclease. *J Mol Biol 228*:243–251.

Crowther R, Blow D. 1967. A method for positioning a known molecule in an unknown crystal structure. *Acta Crystallogr 23*:544–548.

Davis A, Hall A, Williams A. 1988. Charge description of base-catalyzed alcoholysis of aryl phosphodiesters: A ribonuclease model. *J Am Chem Soc 110*:5105–5108.

deMel VS, Martin PD, Doscher MS, Edwards BF. 1992. Structural changes that accompany the reduced catalytic efficiency of two semisynthetic ribonuclease analogs. *J Biol Chem 267*:247–256.

Findlay D, Herries DG, Mathias AP, Rabin BR, Ross CA. 1962. The active site and mechanism of action of bovine pancreatic ribonuclease 7. The catalytic mechanism. *Biochem J 85*:152–153.

Fitzgerald PM. 1988. MERLOT, an integrated package of computer programs for the determination of crystal structures by molecular replacement. *J Appl Crystallogr 21*:273–278.

Gerlt J, Gassman P. 1993. Understanding the rates of certain enzyme-catalysed reactions: Proton abstraction from carbon acids, acyl-transfer reactions, and displacement reactions of phosphodiesters. *Biochemistry 32*:11944–11952.

Gilliland GL, Dill J, Pechik I, Svensson LA, Sjölin L. 1994. The active site of bovine pancreatic ribonuclease: An example of solvent modulated specificity. *Protein Peptide Lett 1*:60–65.

Govil G. 1976. Conformational structure of polynucleotides around the O-P bonds: Refined parameters for CPF calculations. *Biopolymers 15*: 2303–2307.

Haneef I, Moss DS, Stanford MJ, Borkakoti N. 1985. Restrained structure-factor least-squares refinement of protein structures using a vector processing program. *Acta Crystallogr A 41*:426–433.

Heinemann U, Saenger W. 1982. Specific protein–nucleic acid recognition in ribonuclease T1-2′-guanylic acid complex: An X-ray study. *Nature 299*: 27–31.

Heydenreich A, Koellner G, Choe HW, Cordes F, Kisker C, Schindelin H, Adamiak R, Hahn U, Saenger U. 1993. The complex between ribonuclease T1 and 3′GMP suggests geometry of enzymic reaction path. *Eur J Biochem 218*:1005–1012.

Hirs CH, Halmann M, Kycia JH. 1965. Dinitrophenylation and inactivation of bovine pancreatic ribonuclease A. *Arch Biochem Biophys 111*: 209–222.

Jones T. 1985. Interactive computer graphics: FRODO. *Methods Enzymol 115*:157–171.

Karpeisky MY, Yakovlev GI. 1977. Does 3′-cytidine monophosphate bound to ribonuclease A acquire syn-conformation? *FEBS Lett 75*:70–72.

Kim EE, Varadarajan R, Wyckoff HW, Richards FM. 1992. Refinement of the crystal structure of ribonuclease S. Comparison with and between the various ribonuclease A structures. *Biochemistry 31*:12304–12314.

Kraulis P. 1993. MOLSCRIPT: A program to produce both detailed and schematic plots of protein structures. *J Appl Crystallogr 24*:946–950.

Lisgarten J, Zegers I, Gupta V, Maes D, Wyns L, Palmer R, Dealwis C, Aguiler C, Hemmings A. 1993. Structure of the crystalline complex of cytidylic acid (2′-CMP) with ribonuclease at 1.6 Å resolution. Conservation of solvent sites in RNase-A high resolution structures. *Acta Crystallogr D 49*:541–547.

Lisgarten J, Gupta V, Palmer R. 1994. *Acta Crystallogr D*. Forthcoming.

Loris R, Stas P, Wyns L. 1994. Conserved waters in legume lectin crystal structures: The importance of bound water for the sequence-structure relationship within the legume lectin family. *J Biol Chem 269*:26722–26733.

Luzzati V. 1957. Traitement statistique des erreurs dans la détermination des structures cristallines. *Acta Crystallogr 5*:802–810.

Malin R, Zielenkiewicz P, Saenger W. 1991. Structurally conserved water molecules in ribonuclease T1. *J Biol Chem 266*:4848–4852.

Martin PD, Doscher MS, Edwards BF. 1987. The refined crystal structure of a fully active semisynthetic ribonuclease at 1.8-Å resolution. *J Biol Chem 262*:15930–15938.

Messerschmidt A, Pflugrath JW. 1987. Crystal orientation and X-ray pattern prediction routines for area-detector diffraction systems in macromolecular crystallography. *J Appl Crystallogr 20*:306–311.

Meyer E. 1992. Internal water molecules and H-bonding in biological macromolecules: A review of structural features with functional implications. *Protein Sci 1*:1543–1562.

Nachman J, Miller M, Gilliland GL, Carty R, Pincus M, Wlodawer A. 1990. Crystal structure of two covalent nucleoside derivatives of ribonuclease A. *Biochemistry 29*:928–937.

Nonaka T, Nakamura KT, Uesugi S, Ikehara M, Irie M, Mitsui Y. 1993. Crystal structure of RNase MS (as a ribonuclease T1 homologue) complexed with a guanylyl-3′,5′-cytidine analogue. *Biochemistry 32*:11825–11837.

Osterman HL, Walz FG. 1978. Subsites and catalytic mechanism of ribonuclease T1: Kinetic studies using GpA, GpC, GpG, and GpU as substrates. *Biochemistry 17*:4124–4130.

Pavlovsky AG, Borisova SN, Broisov VV, Antonov IV, Karpeisky MY. 1978. The structure of ribonuclease S with fluoride analogue of UpA at 2.5 Å resolution. *FEBS Lett 92*:258–262.

Pletinckx J, Steyaert J, Zegers I, Choe H, Heinemann U, Wyns L. 1994. Crystallographic study of Glu 58 Ala RNase T1 * 2′-guanosine monophosphate at 1.9 Å resolution. *Biochemistry 33*:1654–1662.

Richards FM, Vithayathil PJ. 1959. The preparation of subtilisin-modified ribonuclease and the separation of the protein and peptide components. *J Biol Chem 234*:1459–1464.

Richards FM, Wyckoff HW. 1973. Ribonuclease S. In: Philips DC, Richards FM, eds. *Atlas of molecular structures in biology, vol 1*. Oxford, UK: Clarendon.

Roberts GC, Dennis EA, Meadows DH, Cohen JS, Jardetzky O. 1969. The mechanism of action of ribonuclease. *Proc Natl Acad Sci USA 62*:1151–1158.

Saenger W. 1984. *Principles of nucleic acid structure*. Heidelberg: Springer Verlag.

Santoro J, Gonzalez C, Bruix M, Neira JL, Nieto JL, Herranz J, Rico M.

1993. High-resolution three-dimensional structure of ribonuclease A in solution by nuclear magnetic resonance spectroscopy. *J Mol Biol 229*: 722–734.

Sekharudu C, Sundaralingam M. 1993. Hydration of protein secondary structures—The role in protein folding. In: Westhof E, ed. *Water and biological macromolecules*. London: McMillan Press Ltd. pp 148–162.

Srinivasan A, Yathindra N, Rao V, Prakash S. 1980. Preferred phosphodiester conformations in nucleic acids. A virtual bond torsion potential to estimate lone-pair interactions in a phosphodiester. *Biopolymers 19*: 165–171.

Steyaert J, Hallenga K, Wyns L, Stanssens P. 1990. Histidine-40 of ribonuclease T1 acts as base catalyst when the true catalytic base, glutamic acid-58, is replaced by alanine. *Biochemistry 29*:9064–9072.

Steyaert J, Wyns L, Stanssens P. 1991. Subsite interactions of ribonuclease T1: Viscosity effects indicate that the rate-limiting step of GpN transesterification depends on the nature of N. *Biochemistry 30*:8661–8665.

Takahashi K, Moore S. 1982. Ribonuclease T1. In: Anonymous, eds. *The enzymes, 3rd ed.* New York: Academic Press. pp 435–468.

Tarragona-Fiol A, Eggelte HJ, Habron S, Sanchez E, Taylorson CJ, Ward JM, Rabin BR. 1993. Identification by site-directed mutagenesis of amino acids in the B2 subsite of bovine pancreatic ribonuclease A. *Protein Eng 6*:901–906.

Trautwein K, Holliger P, Stackhouse J, Benner SA. 1991. Site-directed mutagenesis of bovine pancreatic ribonuclease: Lysine-41 and aspartate-121. *FEBS Lett 281*:275–277.

Usher D. 1969. On the mechanism of ribonuclease action. *Proc Natl Acad Sci USA 62*:661–667.

Usher DA, Evelyn S, Erenrich S, Eckstein F. 1972. Geometry of the first step in the action of ribonuclease A. *Proc Natl Acad Sci USA 1*:115–118.

Varadarajan R, Connelly P, Sturtevant J, Richards F. 1992. Heat capacity changes for protein-peptide interactions in the ribonuclease S system. *Biochemistry 31*:1421–1426.

Weber PC, Sheriff S, Ohlendorf DH, Finzel BC, Salemme FR. 1985. The 2-Å resolution structure of a thermostable ribonuclease A chemically crosslinked between lysine residues 7 and 41. *Proc Natl Acad Sci USA 82*:8473–8477.

Williams RL, Greene SM, McPherson A. 1987. The crystal structure of ribonuclease B at 2.5-Å resolution. *J Biol Chem 262*:16020–16031.

Witzel H, Barnard EA. 1962. Mechanism and binding sites in the ribonuclease reaction II. Kinetic studies on the first step of the reaction. *Biochem Biophys Res Commun 7*:295–299.

Wlodawer A. 1984. Structure of bovine pancreatic ribonuclease by X-ray and neutron diffraction. In: Jurnak F, McPherson A, eds. *Biological macromolecules and assemblies, vol II. Nucleic acids and interactive proteins*. New York: Wiley. pp 395–439.

Wlodawer A, Borkakoti N, Moss D, Howlin B. 1986. Comparison of two independently refined models of ribonuclease A. *Acta Crystallogr B 42*: 379–387.

Wlodawer A, Bott R, Sjolin L. 1982. The refined crystal structure of ribonuclease A at 2.0 Å resolution. *J Biol Chem 257*:1325–1332.

Wlodawer A, Miller M, Sjolin L. 1983. Active site of RNase: Neutron diffraction study of a complex with uridine vanadate, a transition-state analog. *Proc Natl Acad Sci USA 80*:3628–3631.

Wlodawer A, Svensson LA, Sjolin L, Gilliland GL. 1988. Structure of phosphate-free ribonuclease A refined at 1.26 Å. *Biochemistry 27*:2705–2717.

Wodak SY, Liu MY, Wyckoff HW. 1977. The structure of cytidilyl(2′,5′)adenosine when bound to pancreatic ribonuclease S. *J Mol Biol 116*:855–875.

Wyckoff HW, Tsernoglou D, Hanson AW, Knox JR, Lee B, Richards FM. 1970. The three-dimensional structure of ribonuclease-S. *J Biol Chem 245*:305–328.

Zegers I, Haikal A, Palmer R, Wyns L. 1994. Crystal structure of RNase T1 with 3′-guanylic acid and guanosine. *J Biol Chem 269*:127–133.